Failure Prognostics of Multilayer Ceramic Capacitors in Temperature-Humidity-Bias Conditions

Jie Gu, *Member, IEEE*, Michael H. Azarian, *Member, IEEE*, and Michael G. Pecht, *Fellow, IEEE*

***Abstract*—This paper presents a prognostics approach which detects the performance degradation of multilayer ceramic capacitors under temperature-humidity-bias conditions, and then predicts remaining useful life. In the tests, three performance parameters (capacitance, dissipation factor and insulation resistance) were monitored in-situ. By comparing the predicted results with the experimental results, the prognostics approach provided advanced warning of failures for capacitors and predicted their remaining useful life.**

***Index Terms*—failure prognostics, health monitoring, multilayer ceramic capacitor**

I. INTRODUCTION

PROGNOSTICS is a process for predicting the future health state of a system by assessing the deviation or degradation from its expected normal conditions [1][2]. There is now a growing interest in predicting the future health of electronics to provide advanced warning of failure, minimize unscheduled maintenance, improve fault identification (including intermittent failures), optimize qualification methods, and enhance the design of future products.

Multilayer ceramic capacitors (MLCCs) are widely used in electronic products to perform functions such as noise reduction (bypass), DC blocking, filtering, timing, tuning, and energy storage. Thus, the health of these capacitors is important for the proper functioning of many electronic products. Previous studies [3][4] have found that multilayer ceramic capacitors (MLCC) exhibit a variety of behaviors during degradation, including parametric drift and intermittent failures. The objective of this study is to develop an approach to detect failures, identify failure precursors, and calculate remaining life.

Physics-of-failure based analysis of electronic products involves evaluation of reliability based on relevant failure mechanisms and failure models. However, it is not always feasible to assign failure mechanisms to a product due to its architectural complexity and insufficient knowledge of the actual application environment. In situations like these, a product's remaining life can be determined by analyzing parameters that indicate the product's performance [4]. By analyzing trends within the data, precursors can be derived from one or more parameters that anticipate the changes that the product will experience in time. With the appropriate selection of precursors, one can extract features from the product that used to better describe the current and future state of health of the product.

Manuscript received May 19, 2008

J. Gu is with the University of Maryland, College Park, MD 20742 USA (phone: 301-405-5324; e-mail: jiegu@calce.umd.edu).

M.H. Azarian is with the University of Maryland, College Park, MD 20742 USA (e-mail: mazarian@calce.umd.edu).

M.G. Pecht is with the University of Maryland, College Park, MD 20742 USA (e-mail: pecht@calce.umd.edu).

II. EXPERIMENTS

In this study, 96 multi-layer ceramic capacitors (MLCC) were selected for in-situ monitoring and life testing in elevated temperature (85°C) and humidity (85% RH) conditions with one of 3 DC voltage bias levels: rated voltage (50 V), low voltage (1.5 V), and no voltage (0 V). Four MLCC types were included, two of which were flexible-termination MLCCs and two were standard-termination MLCCs. For each end-termination type, a group of MLCCs with precious metal electrodes (PME) made of silver-palladium and a group of MLCCs with base metal electrodes (BME) made of nickel were selected. Table 1 summarizes the test conditions and sample sizes for each voltage level used for temperature, humidity, bias (THB) testing of each type of MLCC. Before exposure to the THB condition, the printed circuit boards containing the MLCCs were preconditioned with 20 temperature cycles ranging from -55°C to 125°C with a ramp rate of 5°C/minute and dwell time of 15 minutes at both high and low extremes of temperature. The temperature cycling screening process did not generate any failures.

An electrical circuit was designed for biasing the capacitors during THB testing and measuring their electrical parameters. In this study, the insulation resistance (IR), capacitance (C), and dissipation factor (DF) were monitored in-situ during testing. An LCR meter was used to measure capacitance and dissipation factor. A high resistance meter was used to measure insulation resistance. In order to limit

9778-1-4244-1936-4/08/$25.00 © 2008 IEEE

leakage current in case of capacitor shorting during THB testing, a 1 MΩ resistor was placed in series with each capacitor. In this setup, 96 capacitors were tested together and a multiplexer and datalogger allowed the measurement of electrical parameters for each capacitor once every 200 minutes. The total THB test lasted for around 1240 hours.

Table 1. Test matrix and number of failures of MLCCs during 1240 hours of THB testing at 85°C and 85% RH

Manuf-acturer	End-termination	Electrode Type	Bias (V)	No. of Samples	No. of Insulation Resistance Failures
A	Flexible	PME	50	10	5
A	Flexible	PME	1.5	10	
A	Flexible	PME	0	4	1
B	Flexible	BME	50	10	
B	Flexible	BME	1.5	10	
B	Flexible	BME	0	4	
B	Standard	BME	50	10	
B	Standard	BME	1.5	10	
B	Standard	BME	0	4	
C	Standard	PME	50	10	
C	Standard	PME	1.5	10	
C	Standard	PME	0	4	2
			Sum	96	8

PME: precious metal electrode; BME: base metal electrode

The failure criteria in this study were defined as an IR drop to a value of less than 10^7 Ohms, or a change in capacitance of 10%, or a doubling of the dissipation factor, maintained for five consecutive readings during the THB test. These failure thresholds were consistent with those used in previous studies of MLCCs [4]. In this study, all failures were firstly found by the IR drop. Five consecutive readings were used to prevent erroneous identification of precursors due to noise in the electrical measurements. If the failure did not recover, it was considered a permanent failure; if the failure self-healed later, it was considered a "strong" intermittent failure. And finally, when the IR was less than 10^7 Ohms for fewer than 5 consecutive readings and self-healed later, it was defined as a "weak" intermittent failure. Only permanent failures and "strong" intermittent failures were considered as MLCC failures in this study. The number of observed MLCC failures is summarized in the last column of Table 1.

III. PROGNOSTICS APPROACH

In order simplify the presentation of the prognostics approach, the initial discussion will focus on a subset of the test population that involved ten capacitors from manufacturer A with flexible end-terminations, PME electrode type, and 50V DC bias (shown in the second row of Table 1), since many failures were observed in this group. The results for the remaining capacitors will be summarized at the end of this section.

The prognostics approach used in this study is regression, residual, detection and prediction analysis (RRDP), which shown in Figure 1. The first step was to select the survived capacitors as the training data set. From the training data set, we could calculate the mean and standard deviation for each parameter (IR, C and DF) using Equations (1) and (2). Then the data normalization was performed for each parameter using Equations (3), (4) and (5). Figure 2 to Figure 4 show the normalized values for the five survived capacitors of IR, DF and C respectively. In these figures, the X-axis is the test time for each capacitor (repeated for each of the five capacitors), and the Y axis is the normalized value for IR, C and DF. The figures show the increasing or decreasing trending behaviors. It was also observed that for individual capacitors, parameters C, DF, and IR are correlated with each other, but when all survived capacitors' data are combined together, the sensitivity of the prognostics algorithm to anomalies is reduced. That is because C has different initial values, though its degradation trends are the same. Therefore, in this study when we performed the subsequent regression analysis, we did not use the capacitance (C) data.

$$\mu = \frac{1}{n}\sum_{i=1}^{n} x_i \tag{1}$$

$$\sigma = \sqrt{\frac{\sum_{i=1}^{n}(x_i - \mu)^2}{n-1}} \tag{2}$$

where μ and σ are mean and standard deviation.

$$NIR_i = \frac{IR_i - \mu_{IR}}{\sigma_{IR}} \tag{3}$$

$$NDF_i = \frac{DF_i - \mu_{DF}}{\sigma_{DF}} \tag{4}$$

$$NDC_i = \frac{C_i - \mu_C}{\sigma_C} \tag{5}$$

where IR_i, DF_i, and C_i are i-th sample for IR, DF and C, respectively, and NIR_i, NDF_i, and NC_i are the normalized IR_i, DF_i, and C_i, respectively.

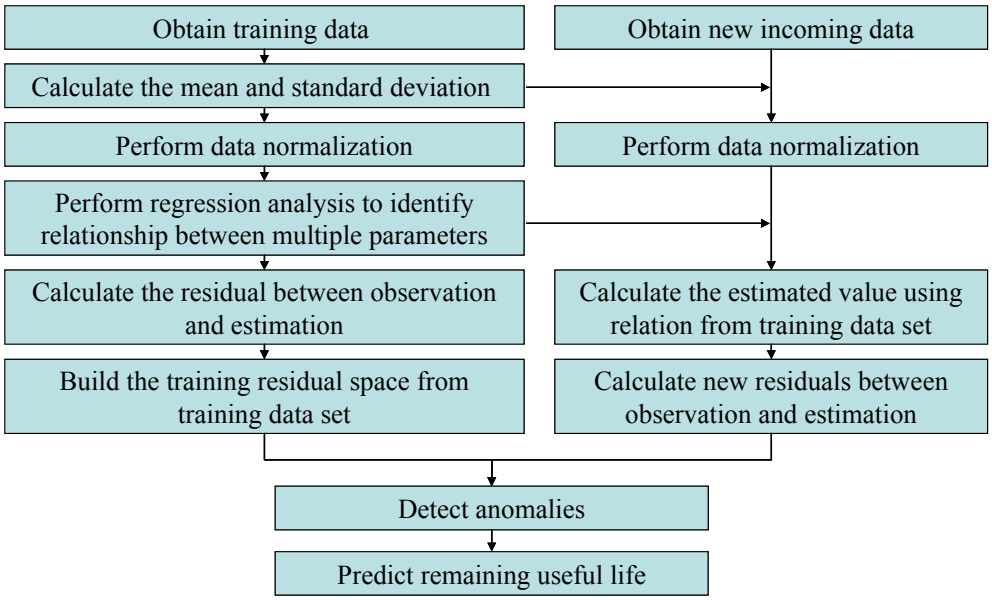

Figure 1. Regression, residual, detection and prediction analysis

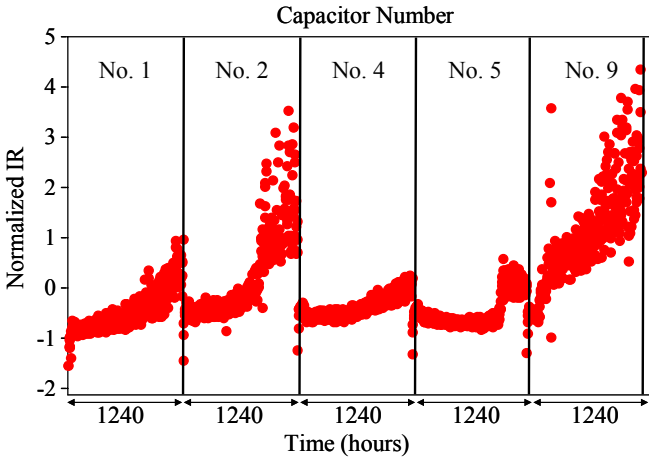

Figure 2. Normalized IR value for five survived capacitors

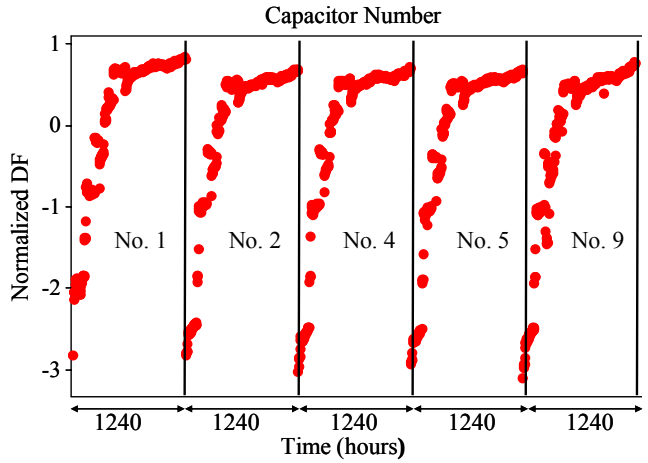

Figure 3. Normalized DF value for five survived capacitors

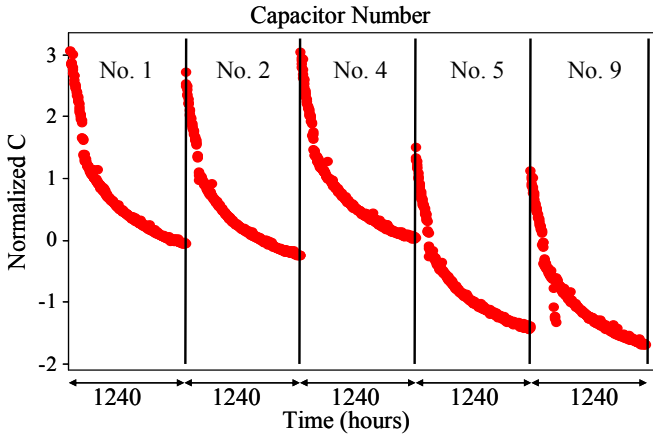

Figure 4. Normalized C value for five survived capacitors

After normalization, regression analysis was performed to build a relationship between the normalized IR (NIR) and the normalized DF (NDF), as shown in Figure 5. Equation (6) shows the regression fit for the relationship between the NIR and the NDF. In addition, 95% confidence bounds for the fit are given in the figure. The upper outliers (outside the upper bound of the 95% confidence interval) represent high values of IR which did not contribute to the capacitor failure, since IR failures only result from a drop in IR, as stated before. Therefore only lower outliers were taken into account. The difference between the dotted and fit lines was recorded as the residual value. When all of the residual values were binned and plotted as a distribution, we could obtain the healthy residual space shown in Figure 6.

When the new incoming IR and DF data were obtained, data normalization was performed using the mean and the standard deviation calculated from the training data set. The estimated NIR was then calculated from the relationship (Equation (6)) obtained from the training data set. After that,

the residual was obtained from the observed NIR and the estimated NIR. By comparing this new residual value with the healthy residual space, it was possible to perform anomaly detection. In Figure 6, a dotted line was marked representing the 95% confidence interval (CI) bound and another representing 99.9% CI bound. If a new residual value was on the left hand side of the 95% bound, it was considered an advanced warning of failure; if the residual was also outside the 99.9% bound, it was defined as an estimated failure.

$$NIR_i = -0.259 + 0.506*NDF_i + 0.442*NDF_i\,\text{^}2 + 0.112*NDF_i\,\text{^}3 \quad (6)$$

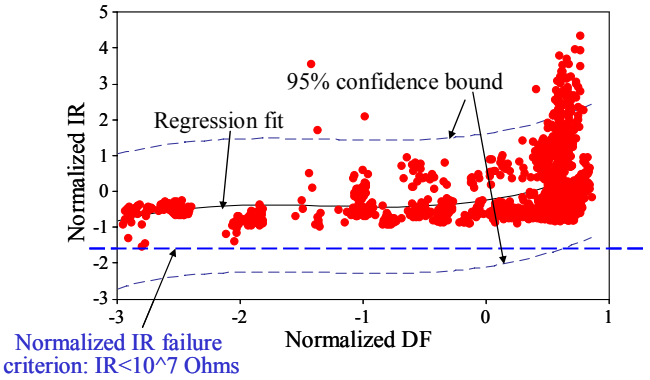

Figure 5. Relationship between NIR and NDF

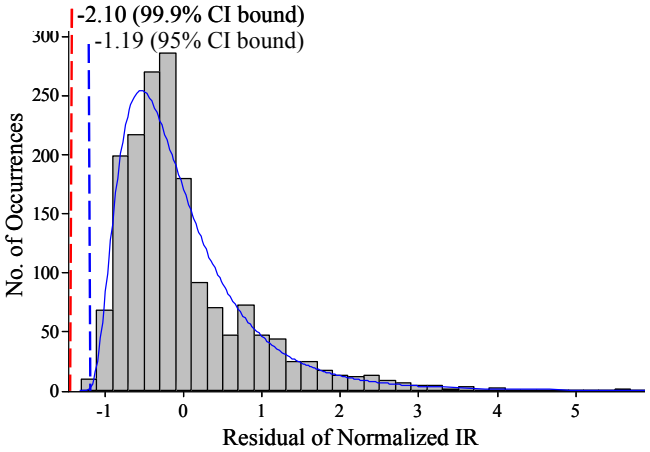

Figure 6. Residual distribution for survived capacitors

Figure 7 shows the degradation trend of the residual value of one failed capacitor (capacitor #3). It gave an advanced warning of failure when the residual value crossed the 95% CI bound at hour 720. The estimated time to failure was when the residual value cross the 99.9% CI bound at hour 806. From the experiment and the failure definition listed in the previous paragraph, the real experimental failure occurred at hour 853.

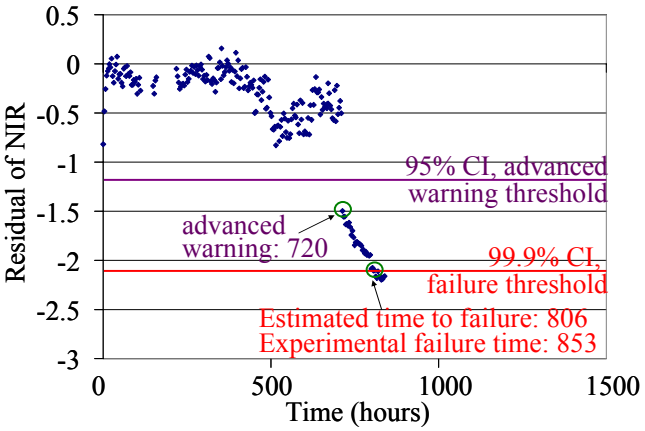

Figure 7. Residual of NIR from failed capacitor #3

From the advanced warning of the estimated failure, the residual value showed a trend that could be used to perform remaining life prediction. The prediction model chosen in this study is referred to as a grey prediction model. The steps used in the grey prediction model are shown in Figure 8 [5][6][7]. The accumulated generating operation (AGO) was used to transform an original set of data into a new set that highlights trends but has less noise. The inverse accumulated generating operation (IAGO) was used to get the inverse data series from the AGO. This was used to transform the forecasted AGO data series back into the original data series. The detailed approach explaining the grey prediction model can be found in references [5][6][7]. Compared with other prediction models, such as the linear, the exponential, and the polynomial prediction models, the grey prediction model gives a more precise and accurate prediction [7]. In addition, assumptions regarding statistical distributions of data are not necessary when applying the grey prediction model. Compared with the auto-regressive (AR) model and the auto-regressive integrated moving average (ARIMA) model, the grey prediction model requires less data to achieve a similar level of accuracy [5]. Also, the grey prediction model regards the newest data as more important than old data. The old data is updated using new data, which produces more accurate results when approaching the actual failure point.

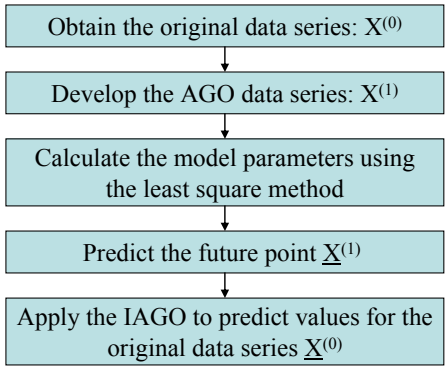

Figure 8. Steps of grey prediction model

The prediction result obtained using the grey prediction model for capacitor #3 is shown in Figure 9. The prediction algorithm was triggered when the residual value crossed the 95% CI line. It used two data above the 95% CI bound and four new incoming data to make the initial prediction. The predicted failure time was hour 753. When new incoming data were obtained, the updated prediction result was more accurate (hour 800).

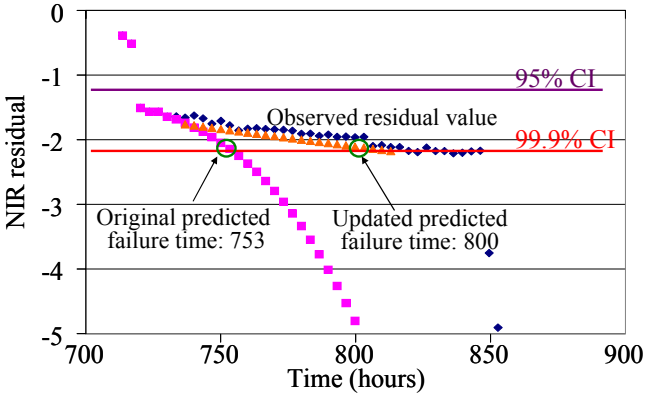

Figure 9. Prediction results for capacitor #3

But in some situations, the advanced warning threshold (95% CI bound) could not provide an early warning since the failure occurred suddenly. One example was capacitor #7, shown in Figure 10 and Figure 11. Before the permanent failure at 1118 hours, capacitor #7 had a total of three advanced warning signals. The first one occurred at hour 853. At the same time, a "strong" intermittent failure of capacitor #7 was observed as the original IR value dropped. From Figure 10, we can see that the failure happened suddenly, and there was no real early warning. One recommendation is to measure the parameters more frequently. If we were to measure the parameters every three seconds rather than every three hours, this might provide an early warning. The second advanced warning signal occurred at hour 939 and quickly recovered. The experiment detected no failure during that time period. The third advanced warning signal occurred at hour 1111, producing an estimated time to failure of 1128 hours. Permanent failure was observed at hour 1118 from experiment.

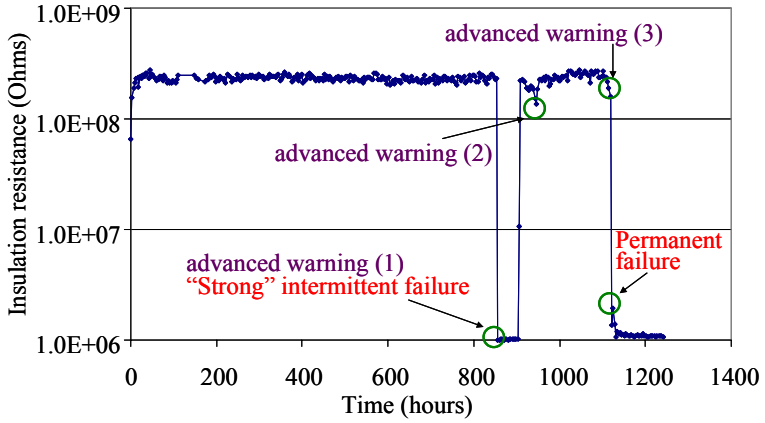

Figure 10. Original IR values recorded from capacitor #7

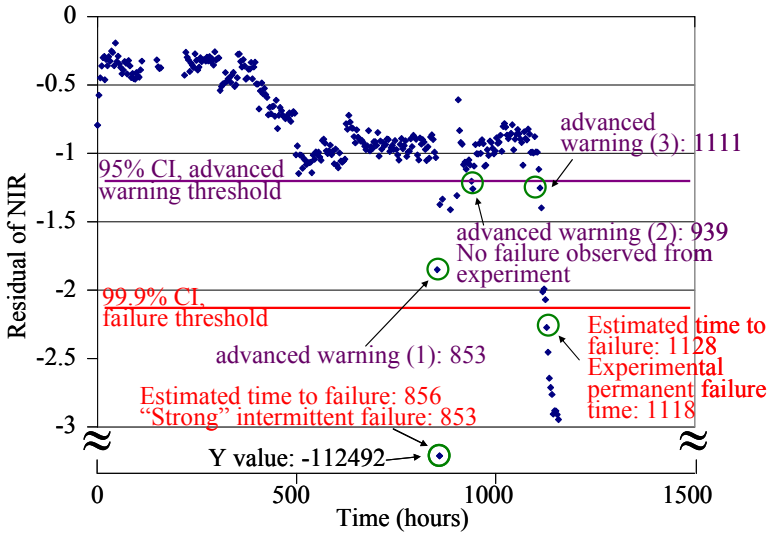

Figure 11. Residual of NIR from failed capacitor #7

All failed capacitors from the subset of ten capacitors are summarized in Table 2. From the table, we can see that among the five failed capacitors, all of the failures can be detected. If the distance from the advanced warning to the real failure is too short, the accuracy of the prediction result is affected.

Table 2. Summary of the first five failed capacitors

Capacitor No.	Time of advanced warning of failure (hours)	Predicted failure time based on grey model before update (hours)	Failure time from experiment (hours)
#3	720	753	853 (permanent failure)
#6	836	883	962 (permanent failure)
#7	853 939 1111	856 Not available 1125	853 ("Strong" intermittent failure) No failure observed 1118 (permanent failure)
#8	317	405	317 ("Strong" intermittent failure)
#10	218	218	218 (permanent failure)

This approach was repeated for all 96 capacitors listed in Table 1, and the results of the tests are summarized in Table 3. It was found that training used to determine the relationship between multiple parameters of capacitors only depended on the capacitor and not on the test conditions (different DC bias). Out of 96 capacitors, the 8 failed capacitors could be detected by residual analysis with no missed alarms. Five out of the eight capacitors that failed gave advanced warning of failure. Among the other 88 survived capacitors, there were eight false alarms. An investigation of the cause of the false alarms found that they shared similar behaviors to that shown in Figure 12: there was one drop of data below 10^7 Ohms, which was defined as a "weak" intermittent failure, but it was not considered a capacitor failure in the study. This means the approach being used provided a conservative result and was highly sensitive in detecting failures.

Table 3. Summary of all 96 capacitors

Manufacturer	Termination	DC bias (V)	No. of samples	No. of failures from experiment	No. of failures detected	No. of existing precursors	No. of false alarms
A	Flexible	50	10	5	5	3	0
		1.5	10	0	0	0	0
		0	4	1	1	0	0
B	Flexible	50	10	0	0	0	0
		1.5	10	0	0	0	0
		0	4	0	0	0	0
B	Standard	50	10	0	0	0	1
		1.5	10	0	0	0	0
		0	4	0	0	0	0
C	Standard	50	10	0	0	0	2
		1.5	10	0	0	0	3
		0	4	2	2	2	2

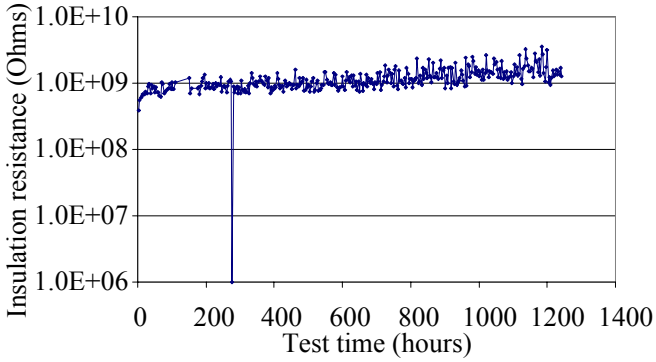

Figure 12. IR recorded for capacitor #70

IV. CONCLUSIONS

A prognostics approach was developed to detect and predict failures using a multi-parameter regression, residual, detection and prediction analysis (RRDP). It showed good promise for detecting failures and providing advanced warning of failure in THB tests of multilayer ceramic capacitors. The healthy residual space was established from the training data set. The new incoming residual values calculated from multiple parameters were compared with the healthy residual space for anomaly detection. The grey prediction model was then used to perform a remaining life calculation.

The study presented in this paper found that the training process for the prognostics approach depended only on the capacitor type, and not on the test conditions (such as different DC bias levels). For 8 failed capacitors out of the 96 capacitors, all failures could be detected with no missed alarms. 5 out of the 8 failed capacitors yielded advanced warning of failure. In addition, a further 8 out of the 96 capacitors were observed to have false alarms, which were normally caused by "weak" intermittent failures.

REFERENCES

[1] N. Vichare, and M.G. Pecht, "Prognostics and Health Management of Electronics," *IEEE Transactions on Components and Packaging Technologies*, Vol. 29, No. 1, March 2006, pp. 222–229.

[2] M.G. Pecht, *Prognostics and Health Management of Electronics*, Wiley-Interscience, NY, USA, 2008.

[3] M. Keimasi, M.H. Azarian, and M.G. Pecht, "Isothermal Aging Effects on Flex Cracking of Multilayer Ceramic Capacitors with Standard and Flexible Terminations", *Microelectronics Reliability*, 2007, Vol. 47, pp. 2215-2225.

[4] L. Nie, M.H. Azarian, M. Keimasi, and M.G. Pecht, "Prognostics of Ceramic Capacitor Temperature-Humidity-Bias Reliability Using Mahalanobis Distance Analysis," *Circuit World*, 2007, Vol. 33, No.3, pp. 21-28.

[5] J.L. Deng, "The Control Problems of Grey Systems", *Journal of Systems and Control Letters*, 1982, Vol. 1, No. 5, pp.288-294.

[6] S.F. Liu, and Y. Lin, *Grey Information: Theory and Practical Applications*, Springer, London, UK, 2006.

[7] T.H.M. El-Fouly, E.F. El-Saadany, and M.M.A. Salama, "Grey Prediction for Wind Energy Conversion Systems Output Power Prediction", *IEEE Transactions on Power Systems*, Aug. 2006, Vol. 21, No. 3, pp. 1450-1452.

[8] J.L. Deng, "Introduction to Grey System Theory", *Journal of Grey System*, 1989, Vol. 1, No. 1, pp. 1-24.

Jie Gu (M' 05) received the B.S. degree in mechanical engineering from the University of Science and Technology in China, and the M.S. degree in Mechanical Engineering from the National University of Singapore. He is an IEEE student member, and currently a Ph.D. student in mechanical engineering at the University of Maryland, College Park, in the area of electronic prognostics and health management.

Michael H. Azarian (M' 96) is a research scientist at CALCE at the University of Maryland. He holds a Ph.D. in Materials Science and Engineering from Carnegie Mellon University, a Masters degree in Metallurgical Engineering and Materials Science from Carnegie Mellon, and a Bachelors degree in Chemical Engineering from Princeton University. His research on reliability of electronic products has led to publications on electrochemical migration, capacitor reliability, electronic packaging, and tribology. He holds 5 US patents for inventions in data storage and contamination control. Before joining CALCE, he spent 13 years in the data storage, advanced materials, and fiber optics industries

Michael G. Pecht (F' 92) is a Chair Professor and the Director of the CALCE Electronic Products and Systems Center and the Center for Prognostics and Health Management at the University of Maryland. Dr. Pecht has an M.S. in Electrical Engineering and an M.S. and Ph.D. in Engineering Mechanics from the University of Wisconsin at Madison. He is a Professional Engineer, an IEEE Fellow, an ASME Fellow, and a Westinghouse Fellow. He has written eleven books on electronics products development. He has written six books on the electronics industry in S.E. Asia. He served as chief editor of the IEEE Transactions on Reliability for eight years and on the advisory board of IEEE Spectrum. He is currently the chief editor for Microelectronics Reliability. He serves as a consultant for various companies, providing expertise in strategic planning, design, test, and risk assessment of electronic products and systems.